10.1098/rsta.2003.1210

THE ROYAL SOCIETY

# Coherent cold collisions with neutral atoms in optical lattices

By Immanuel Bloch, Markus Greiner, Olaf Mandel and Theodor W. Hänsch

*Ludwig-Maximilians-Universität, Schellingstraße 4/III, 80799 Munich, Germany and Max-Planck-Institut für Quantenoptik, Hans-Kopfermann-Straße 1, 85748 Garching, Germany*

*Published online 2 June 2003*

By loading a Bose–Einstein condensate into a three-dimensional optical lattice potential, we have been able to demonstrate several fundamental aspects of coherent cold collisions between neutral atoms. We show experimentally how such collisions lead to a well-defined phase shift in the corresponding many-body wave function. The experimental realization of such interactions can be fundamental for the simulation of complex condensed-matter-physics Hamiltonians, for the creation of large-scale entanglement and for the realization of quantum gates with neutral atoms.

**Keywords: Bose–Einstein condensation; ultracold atoms; optical lattices; quantum computation**

## 1. Introduction

Over the last seven years, spectacular experiments with atomic Bose–Einstein condensates (BECs) have demonstrated the remarkable wave-like nature of this new form of matter. A BEC can be considered as the perfect realization of a classical matter wave, just as the emitted light from a laser is the perfect realization of a classical electromagnetic wave. However, a quantized field underlies the classical matter wave of a BEC and it is therefore natural to ask whether one can observe effects due to such a quantization.

Here we briefly summarize our experimental results on BECs in optical lattices that are relevant for quantum information processing. After starting with a gaseous atomic BEC, we superimpose a three-dimensional periodic optical lattice potential on top of it. There the atoms are trapped in an array of thousands of microscopic trapping potentials due to the optical dipole force potential. By increasing the lattice potential depth we are able to drive such a many-body system through a Mott insulating transition (Fisher *et al*. 1989; Jaksch *et al*. 1998; Greiner *et al*. 2002*a*). A Mott insulator provides an ideal environment for quantum information processing. When the relevant parameters such as density and the external harmonic confinement are tuned to the right value, a large region of the optical lattice can be filled with

One contribution of 20 to a Discussion Meeting 'Practical realizations of quantum information processing'.

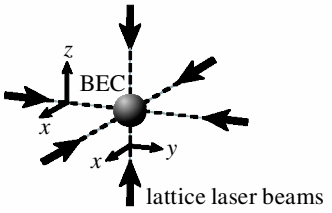


Figure 1. Three orthogonal standing waves are overlapped at the position of the BEC to create a three-dimensional periodic potential with simple cubic-lattice structure.

exactly one atom per lattice. The Mott transition can therefore be employed to initialize a quantum register, where each qubit is formed by a single neutral atom on a lattice site, with up to $10^5$ sites being occupied.

In order to realize quantum gates with neutral atoms in optical lattices, several schemes have been proposed (Brennen *et al*. 1999; Jaksch *et al*. 1999; Jané *et al*. 2002; Sorenson & Molmers 1999, 2001; Briegel *et al*. 2000). In one of the most prominent ones, controlled cold collisions between neutral atoms have been suggested (Jaksch *et al*. 1999). Here collisions between ground-state atoms lead to a well-defined phase-shift in the corresponding many-body state that can be used for quantum logic gates. By first preparing the atoms to be in a superposition of different number states on a single lattice site and then observing the subsequent dynamics of the many-body system, we directly prove the full coherence of such cold collisions.

## 2. Superfluid to Mott insulator transition

### (*a*) *Experimental set-up*

The starting point for all the experiments is magnetically trapped BECs of $^{87}$Rb atoms in a new experimental set-up with excellent optical access (Greiner *et al*. 2002*a*). In order to create a three-dimensional periodic potential we overlap the crossing point of three optical standing waves at the position of the BEC (see figure 1). These standing waves are operated at a wavelength of $\lambda = 830$–$850$ nm such that they are red detuned relative to the Rb D1- and D2-atomic resonances. Due to the resulting dipole force (Grimm *et al*. 2000), the atoms are attracted to the intensity maxima of the light field such that a periodic potential is realized through the optical interference pattern. This periodic potential has a simple cubic-lattice structure with a lattice spacing of $\lambda/2$. The potential depth of the optical lattice is naturally measured in units of the recoil energy $E_\mathrm{r} = \hbar^2k^2/2m$, with $k$ being the wave vector of the laser light $k = 2\pi/\lambda$ and $m$ being the mass of a single atom. All laser beams are intensity stabilized to provide stable optical potentials during and between different realizations of the experiment. In our set-up, lattice potential depths of up to $45E_\mathrm{r}$ can be realized, leading to vibrational frequencies of up to 40 kHz on each lattice site.

### (*b*) *Bose–Hubbard Hamiltonian*

The behaviour of bosonic atoms with repulsive interactions in a periodic potential is fully captured by the Bose–Hubbard Hamiltonian of solid-state physics, which in

the homogeneous case can be expressed through

$$H = -J \sum_{\langle i,j \rangle} \hat{a}_i^\dagger \hat{a}_j + \tfrac{1}{2} U \sum_i \hat{n}_i(\hat{n}_i - 1). \tag{2.1}$$

Here $\hat{a}_i^\dagger$ and $\hat{a}_i$ describe the creation and annihilation operators for a boson on the $i$th lattice site and $\hat{n}_i$ counts the number of bosons on the $i$th lattice site. The tunnel coupling between neighbouring potential wells is characterized by the tunnel matrix element

$$J = -\int \mathrm{d}^3x\, w(\boldsymbol{x} - \boldsymbol{x}_i)\left(\frac{-\hbar^2\nabla^2}{2m} + V_{\mathrm{lat}}(\boldsymbol{x})\right) w(\boldsymbol{x} - \boldsymbol{x}_j),$$

where $w(\boldsymbol{x} - \boldsymbol{x}_i)$ is a single-particle Wannier function localized to the $i$th lattice site and $V_{\mathrm{lat}}(\boldsymbol{x})$ indicates the optical lattice potential. The repulsion between two atoms on a single lattice site is quantified by the on-site matrix element $U = (4\pi\hbar^2 a/m) \int |w(\boldsymbol{x})|^4 \, \mathrm{d}^3x$, with $a$ being the scattering length of an atom. Due to the short range of the interactions compared with the lattice spacing, the interaction energy is well described by the second term of equation (2.1), which characterizes a purely on-site interaction.

### (*c*) *Ground states of the Bose–Hubbard Hamiltonian*

The Bose–Hubbard Hamiltonian of equation (2.1) has two distinct ground states depending on the strength of the interactions $U$ relative to the tunnel-coupling $J$. For $U/J \ll 1$ the tunnelling term dominates the Hamiltonian and the ground-state of the many-body system with $N$ atoms is given by a product of identical single-particle Bloch waves, where each atom is spread out over the entire lattice with $M$ lattice sites

$$|\Psi_{\mathrm{SF}}\rangle_{U/J \approx 0} \propto \left(\sum_{i=1}^{M} \hat{a}_i^\dagger\right)^N |0\rangle \approx \prod_{i=1}^{M} |\phi\rangle_i. \tag{2.2}$$

Here the single-site many-body wave function $|\phi\rangle_i$ is almost equivalent to a coherent state. The atom number per lattice site then remains uncertain and follows a Poissonian distribution with a variance given by the average number of atoms on this lattice site $\mathrm{var}(n_i) = \langle \hat{n}_i \rangle$. The non-vanishing expectation value of $\psi_i = \langle \phi_i | \hat{a}_i | \phi_i \rangle$ then characterizes the coherent matter-wave field on the $i$th lattice site. This matter-wave field has a fixed phase relative to all other coherent matter-wave fields on different lattice sites.

If, on the other hand, interactions dominate the behaviour of the Hamiltonian, such that $U/J \gg 1$, then fluctuations in the atom number on a single lattice site become energetically costly and the ground state of the system will instead consist of localized atomic wave functions that minimize the interaction energy. The many-body ground state is then a product of local Fock states for each lattice site. In this limit the ground state of the many-body system for a commensurate filling of $n$ atoms per lattice site is given by

$$|\Psi_{\mathrm{MI}}\rangle_{J \approx 0} \propto \prod_{i=1}^{M} (\hat{a}_i^\dagger)^n |0\rangle. \tag{2.3}$$

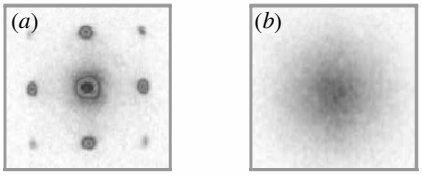


Figure 2. Absorption images of multiple matter-wave interference patterns after releasing the atoms from an optical lattice potential with a potential depth of (*a*) $7E_{\mathrm{r}}$ and (*b*) $20E_{\mathrm{r}}$. The ballistic expansion time was 15 ms.

In such a situation the atom number on each lattice site is ideally exactly determined but the phase of the coherent matter-wave field on a lattice site has obtained a maximum uncertainty. This is characterized by the disappearance of the matter-wave field on the $i$th lattice site, $\psi_i = \langle\phi_i|\hat{a}_i|\phi_i\rangle \approx 0$.

### (*d*) *Superfluid–Mott insulator transition*

In the experiment the crucial parameter $U/J$ that characterizes the strength of the interactions relative to the tunnel coupling between neighbouring sites can be varied by simply changing the potential depth of the optical lattice potential. By increasing the lattice potential depth, $U$ increases almost linearly, due to the tighter localization of the atomic wave packets on each lattice site and $J$ decreases exponentially due the decreasing tunnel coupling. The ratio $U/J$ can therefore be varied over a large range from $U/J \approx 0$ up to values in our case of $U/J \approx 2000$.

In the superfluid regime (Cataliotti *et al.* 2001), phase coherence of the matter-wave field across the lattice characterizes the many-body state. This can be observed by suddenly turning off all trapping fields, such that the individual matter-wave fields on different lattice sites expand and interfere with each other. After a fixed time-of-flight period, the atomic density distribution can then be measured by absorption imaging. Such an image directly reveals the momentum distribution of the trapped atoms. In figure 2*a* an interference pattern can be seen after releasing the atoms from a three-dimensional lattice potential.

If on the other hand the optical lattice potential depth is increased such that the system is in the Mott insulating regime, phase coherence is lost between the matter-wave fields on neighbouring lattice sites due to the formation of Fock states (Jaksch *et al.* 1998; Fisher *et al.* 1989; Sachdev 2001). In this case no interference pattern can be seen in the time-of-flight images (see figure 2*b*).

In addition to the fundamentally different momentum distributions in the superfluid and Mott insulating regime, the excitation spectrum is also markedly different in both cases. Whereas the excitation spectrum in the superfluid regime is gapless, it is gapped in the Mott insulating regime. This energy gap of order $U$ can be attributed to the now localized atomic wave functions of the atoms.

## 3. Collapse and revival of the matter-wave field of a BEC

Whenever a condensate is split into two parts such that a fixed relative phase is established between those two parts, the many-body state in each of the BECs is in a superposition of different atom-number states. Let us now consider the case of repulsive interactions between the atoms and determine how such superpositions of

atom-number states evolve over time, taking into account the collisions between the atoms. Let us first assume that all atoms in a subsystem occupy the ground state of its external confining potential. If the interaction energy is then small compared with the vibrational spacing in this potential well, the Hamiltonian governing the behaviour of the atoms is given by

$$H = \tfrac{1}{2}U\hat{n}(\hat{n}-1). \tag{3.1}$$

The eigenstates of the above Hamiltonian are Fock states $|n\rangle$ in the atom number, with eigenenergies $E_n = Un(n-1)/2$. The evolution with time of such an $n$-particle state is then simply given by $|n\rangle(t) = |n\rangle(0) \times \exp(-\mathrm{i}E_n t/\hbar)$.

If the atoms in such a subsystem are brought into a superposition of atom-number states $|n\rangle$, which always occurs whenever a fixed relative phase persists between the two subsystems, each subsystem is in a superposition of eigenstates $|n\rangle$, which results in a dynamical evolution of this state over time. Let us consider for example a coherent state

$$|\alpha\rangle = \exp(-\tfrac{1}{2}|\alpha|^2)\sum_n \frac{\alpha^n}{\sqrt{n!}}|n\rangle$$

in each subsystem (Walls & Milburn 1994). Here $\alpha$ is the amplitude of the coherent state with $|\alpha|^2$ corresponding to the average atom number in the subsystem. The evolution with time of such a coherent state can be evaluated by taking into account the time evolution of the different Fock states forming the coherent state

$$|\alpha\rangle(t) = \exp(-\tfrac{1}{2}|\alpha|^2)\sum_n \frac{\alpha^n}{\sqrt{n!}}\exp(-\mathrm{i}Un(n-1)t/2\hbar)|n\rangle. \tag{3.2}$$

The coherent matter-wave field $\psi$ in each of the subsystems can then simply be evaluated through $\psi = \langle\alpha(t)|\hat{a}|\alpha(t)\rangle$, which exhibits an intriguing dynamical evolution (Wright *et al.* 1996; Imamoglu *et al.* 1997; Castin & Dalibard 1997; Dunningham *et al.* 1998). At first, the different phase evolutions of the atom-number states lead to a collapse of $\psi$. However, at integer multiples in time of $h/U$, all phase factors in the above equation re-phase modulo $2\pi$ and thus lead to a revival of the initial coherent state (see also figure 3). The collapse and revival of the coherent matter-wave field of a BEC is reminiscent of the collapse and revival of the Rabi oscillations in the interaction of a single atom with a single-mode electromagnetic field in cavity quantum electrodynamics (Rempe *et al.* 1987; Brune *et al.* 1996). There, the nonlinear atom–field interaction induces the collapse and revival of the Rabi oscillations, whereas here the nonlinearity due to the interactions between the atoms themselves leads to the series of collapses and revivals of the matter-wave field. It should be pointed out that such a behaviour has also been theoretically predicted to occur for a coherent light field propagating in a nonlinear medium (Yurke & Stoler 1986) but to our knowledge has never been observed experimentally.

In order to realize a coherent state in a potential well, we again use the optical lattice potential and ramp it to a potential depth $V_{\mathrm{A}}$, which is still completely in the superfluid regime. Then, for low lattice depths, the many-body state in each potential well is almost equal to that of a coherent state with a corresponding average atom number. In such a situation the phase of the matter-wave field on the $i$th lattice site is fixed relative to the matter-wave fields on the other lattice sites. Then, in order to isolate the wells from each other, we rapidly increase the lattice potential

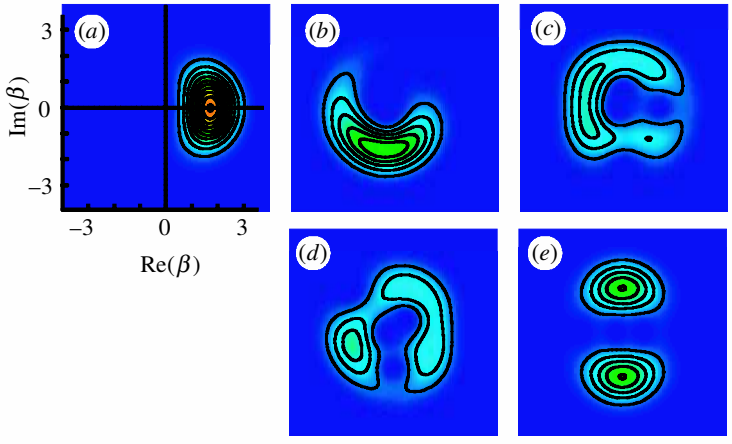


Figure 3. Calculated quantum dynamics of an initially slightly number-squeezed state with an average number of three atoms. Such a state, where the sub-Poissonian character of the many-body state is characterized by $0 < g < 1$, can be parametrized as $|\alpha\rangle(t) \propto \sum_n g^{n(n-1)} \times (\alpha^n/\sqrt{n!}) \exp(-\mathrm{i}n(n-1)t/2\hbar)|n\rangle$. In the graph $g = 0.8$. The dynamical evolution of the quantum state is caused by the coherent cold collisions between the atoms. The graphs show the overlap of the dynamically evolved input state with an arbitrary coherent state of amplitude $\beta$. Evolution times are (*a*) $0h/U$; (*b*) $\frac{1}{8}h/U$; (*c*) $\frac{1}{4}h/U$; (*d*) $\frac{3}{8}h/U$; and (*e*) $\frac{1}{2}h/U$.

depth to $V_{\mathrm{B}}$ with negligible tunnel coupling on a time-scale that is fast compared with the tunnelling time $h/J$ in the system. Thereby the atoms do not have time to redistribute themselves during the ramp-up of the optical potential and we preserve the initial atom-number distribution on each lattice site. On the other hand, the time-scale is slow compared with the oscillation frequencies on each lattice site such that no vibrational excitations are created in the ramp-up process and all atoms remain in the vibrational ground state of each well. Using this method, we are able to freeze out the atom-number distribution at a potential depth $V_{\mathrm{A}}$ and the dynamics of each of the matter-wave fields on different lattice sites is now governed by the Hamiltonian of equation (3.1).

We then follow the dynamical evolution of the matter-wave fields by holding the atoms at the lattice potential depth $V_{\mathrm{B}}$ for a variable hold time and then releasing them suddenly from the combined optical and magnetic trapping potentials. After a suitable time-of-flight period we then take absorption images of the multiple matter-wave interference pattern (see figure 4). Initially, directly after ramping up the lattice potential, the interference pattern is clearly visible; however, after *ca.* 250 μs the interference pattern is completely lost. Here the disappearance of the interference pattern is caused by the collapse of the matter-wave fields on each lattice site. But, after a total hold time of 550 μs, the original interference pattern is regained again, showing that the matter-wave fields have revived. It is important to note that the atom-number statistics in each of the wells remains constant throughout the dynamical evolution time. This is fundamentally different from the disappearance of the interference pattern in the Mott insulator case, where the atom-number distribution changes, but no further dynamical evolution occurs.

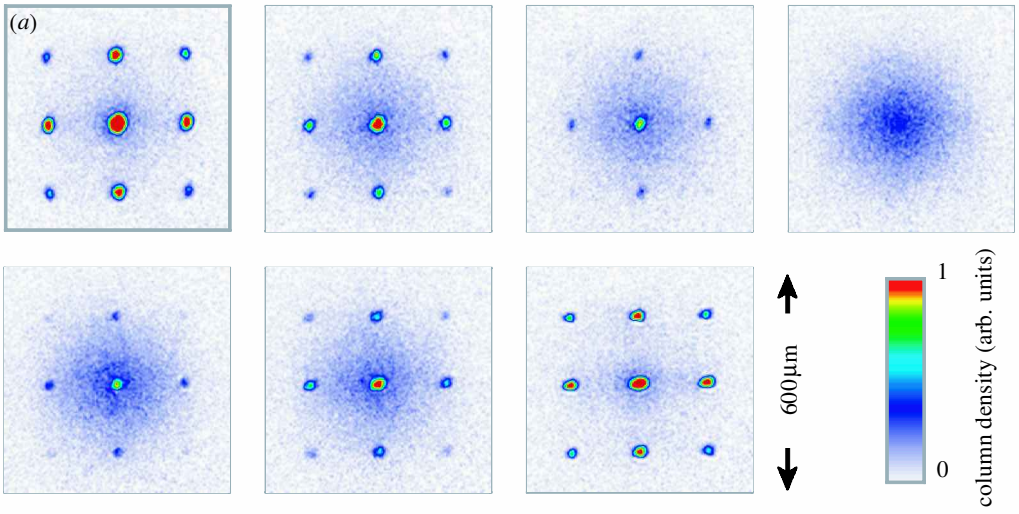


Figure 4. Dynamical evolution of the multiple matter-wave interference pattern after jumping from a potential depth $V_A = 8E_r$ to a potential depth $V_B = 22E_r$ and a subsequent hold time $\tau$. Hold times $\tau$: (*a*) 0 µs; (*b*) 100 µs; (*c*) 150 µs; (*d*) 250 µs; (*e*) 350 µs; (*f*) 400 µs and (*g*) 550 µs.

## 4. Conclusion

With the above experiments, two crucial aspects for quantum information processing with neutral atoms have been demonstrated. First, the Mott-insulator transition can be used to efficiently initialize a large atomic qubit register. Furthermore, the experiment on the collapse and revival of the matter-wave field of a BEC demonstrates that the collisions between vibrational ground-state atoms can be efficiently used to induce controlled phase shifts in the atomic many-body state. Together with schemes for a spin dependent transport of neutral atoms in optical lattices, interactions between atoms on neighbouring lattice sites should be realizable in the near future. Such controlled interactions between atoms on neighbouring lattice sites could be used to create highly entangled many-body states (Jaksch *et al.* 1999; Briegel & Raussendorf 2001) that could form the basis for a neutral-atom quantum computer (Briegel *et al.* 2000; Raussendorf & Briegel 2001).

## References

Brennen, G., Caves, C. M., Jessen, P. S. & Deutsch, I. H. 1999 Quantum logic gates in optical lattices. *Phys. Rev. Lett.* **82**, 1060–1063.

Briegel, H. J. & Raussendorf, R. 2001 Persistent entanglement in arrays of interacting particles. *Phys. Rev. Lett.* **86**, 910–913.

Briegel, H. J., Calarco, T., Jaksch, D., Cirac, J. I. & Zoller, P. 2000 Quantum computing with neutral atoms in optical lattices. *J. Mod. Opt.* **47**, 415–451.

Brune, M., Schmidt-Kaler, F., Maali, A., Dreyer, J., Hagley, E., Raimond, J. M. & Haroche, S. 1996 Quantum Rabi oscillations: a direct test of field quantization in a cavity. *Phys. Rev. Lett.* **76**, 1800–1803.

Castin, Y. & Dalibard, J. 1997 Relative phase of two Bose–Einstein condensates. *Phys. Rev.* A **55**, 4330–4337.

Cataliotti, F. S., Burger, S., Fort, C., Maddaloni, P., Minardi, F., Trombettoni, A., Smerzi, A. & Inguscio, M. 2001 Josephson junction arrays with Bose–Einstein condensates. *Science* **293**, 843–836.

Dunningham, J. A., Collett, M. J. & Walls, D. F. 1998 Quantum states of a trapped Bose–Einstein condensate. *Phys. Lett.* A **245**, 49–54.

Fisher, M. P. A., Weichman, P. B., Grinstein, G. & Fisher, D. S. 1989 Boson localization and the superfluid–insulator transition. *Phys. Rev.* B **40**, 546–570.

Greiner, M., Mandel, O., Esslinger, T., Hänsch, T. W. & Bloch, I. 2002*a* Quantum phase transition from a superfluid to a Mott insulator in an ultracold gas of atoms. *Nature* **415**, 39–44.

Greiner, M., Mandel, O., Hänsch, T. W. & Bloch, I. 2002*b* Collapse and revival of the matter wave field of a Bose–Einstein condensate. *Nature* **419**, 51–54.

Grimm, R., Weidemüller, M. & Ovchinnikov, Yu. B. 2000 Optical dipole traps for neutral atoms. *Adv. Atom. Mol. Opt. Phys.* **42**, 95.

Imamoglu, A., Lewenstein, M. & You, L. 1997 Inhibition of coherence in trapped Bose–Einstein condensates. *Phys. Rev. Lett.* **78**, 2511–2514.

Jaksch, D., Bruder, C., Cirac, J. I., Gardiner, C. W. & Zoller, P. 1998 Cold bosonic atoms in optical lattices. *Phys. Rev. Lett.* **81**, 3108–3111.

Jaksch, D., Briegel, H. J., Cirac, J. I., Gardiner, C. W. & Zoller, P. 1999 Entanglement of atoms via cold controlled collisions. *Phys. Rev. Lett.* **82**, 1975–1978.

Jané, E., Vidal, G., Duer, W., Zoller, P. & Cirac, J. I. 2002 Simulation of quantum dynamics with quantum optical systems. *Quant. Informat. Computat.* **3**, 15–37.

Raussendorf, R. & Briegel, H. J. 2001 A one-way quantum computer. *Phys. Rev. Lett.* **86**, 5188–5191.

Rempe, G., Walther, H. & Klein, N. 1987 Observation of quantum collapse and revival in a one-atom maser. *Phys. Rev. Lett.* **58**, 353–356.

Sachdev, S. 2001 *Quantum phase transitions*. Cambridge University Press.

Sorenson, A. & Molmer, K. 1999 Spin–spin interaction and spin squeezing in optical lattices. *Phys. Rev. Lett.* **83**, 2274–2278.

Sorenson, A. & Molmer, K. 2001 Entanglement and extreme spin squeezing. *Phys. Rev. Lett.* **86**, 4431–4434.

Walls, D. F. & Milburn, G. J. 1994 *Quantum optics*. Springer.

Wright, E. M., Walls, D. F. & Garrison, J. C. 1996 Collapses and revivals of Bose–Einstein condesates formed in small atomic samples. *Phys. Rev. Lett.* **77**, 2158–2161.

Yurke, B. & Stoler, D. 1986 Generating quantum-mechanical superpositions of macroscopically distinguishable states via amplitude dispersion. *Phys. Rev. Lett.* **57**, 13–16.